Journal of Advanced Concrete Technology
Materials, Structures and Environment

Bio-based self-healing mortar: An experimental and numerical study

Eirini Tziviloglou, Zichao Pan, Henk M Jonkers, Erik Schlangen

Journal of Advanced Concrete Technology, volume 15 (2017), pp. 536-543

Scientific paper

Bio-based Self-healing Mortar: An Experimental and Numerical Study

Eirini Tziviloglou[1*], Zichao Pan[2], Henk M. Jonkers[3] and Erik Schlangen[4]

Received 16 February 2017, accepted 29 August 2017 doi:10.3151/jact.15.536

Abstract

Self-healing concrete can repair itself by closing micro-cracks and thus protect itself from ingress of deleterious gasses and liquids that can affect its durability. Many self-healing concepts have been developed in the recent years which target on the recovery of water tightness after cracking. Among those systems, the bio-based healing agents have shown promising results regarding the crack sealing performance. This paper studies the crack sealing efficiency of bio-based healing mortar with expanded clay particles. The investigation of sealing performance is conducted through experimental and computational approaches. Image processing and crack permeability test results are compared with results obtained by computer simulations. The study reveals that the experimental approaches might overestimate the crack closure percentage, while the computer simulation mostly underestimates the crack sealing. Finally, recommendations are given to improve the results obtained by both methodologies.

1. Introduction

Cracking in concrete can highly influence its durability and affect the life span of a structure (Schlangen *et al.* 2009). Design codes indicate maximum allowable crack widths based on empirical studies (Pacheco *et al.* 2014). To minimize the risk of reinforcement corrosion, Eurocode 2 recommends that the maximum crack width for mild environments should be 0.4 mm and 0.2 mm for more aggressive exposure classes. Design calculations indicate that the larger cover depths will result in enhanced durability. Yet, self-healing concrete is an alternative solution to succeed increased durability without the need to over-dimension and thus to increase the total cost of a structure.

In self-healing concrete, the intrinsic ability of cementitious materials to seal micro-cracks (up to 0.2 mm) due to prolonged hydration, carbonation of matrix etc. (Hearn 1998; Edvardsen 1999; ter Heide 2005) is improved by adding the healing agent. The healing agent upon cracking is released and fills the crack volume. By this means the inner part of the structure is protected and thus the danger of reinforcement corrosion is minimized. Many self-healing concepts have been developed in the recent years using various types of healing agents (Schlangen *et al.* 2009; de Rooij *et al.* 2013).

Among those systems, the bio-based healing agents are of great scientific interest, since they have two advantageous points over other healing agents. First, the bio-based healing agents usually contain less synthetic compounds. In addition, they have another significant characteristic, namely the prolonged lifetime and the possibility of repeated use. The biological healing agents do not “expire” and can be re-activated in the future upon further cracking. Consequently, the whole concept is oriented to increase sustainability and reduce costs.

The research of self-healing in cementitious materials often focuses on laboratory and experimental work (Zemskov *et al.* 2011). Experimental studies are very useful to test and evaluate each self-healing concept and its functionality. There are various ways to examine the degree of self-healing such as: visual observation (Wiktor *et al.* 2011; Van Tittelboom *et al.* 2012; Palin *et al.* 2015; Roig-Flores *et al.* 2015), crack absorption tests (Wang *et al.* 2012;, Feiteira *et al.* 2016), crack permeability tests (Edvardsen 1999; Reinhardt *et al.* 2003; Jonkers 2011; Sangadji 2015; Tziviloglou *et al.* 2016), acoustic emission tests (Van Tittelboom *et al.* 2012; Feiteira *et al.* 2016; Malm *et al.* 2016) etc. However, there are few publications that include modelling studies regarding self-healing in cementitious materials (Joseph 2008; Huang *et al.* 2012; Hilloulin *et al.* 2016) and even fewer related to bio-based self-healing concrete (Zemskov *et al.* 2011).

The current paper focuses on the study of the bio-based self-healing mortar, where the healing agent is embedded in lightweight aggregates (LWA). Upon crack formation, the weak lightweight capsules break; the healing agent activates and fills the open crack by precipitating calcium carbonate ($CaCO_3$). The aim of this study is to investigate the crack closure on mortar

[1]PhD Candidate, Faculty of Civil Engineering and Geosciences, Delft University of Technology, Delft, The Netherlands. *Corresponding author,
E-mail: E.Tziviloglou@tudelft.nl
[2]Assistant Professor, Department of Bridge Engineering, Tongji University, Shanghai, China.
[3]Associate Professor, Faculty of Civil Engineering and Geosciences, Delft University of Technology, Delft, The Netherlands.
[4]Professor, Faculty of Civil Engineering and Geosciences, Delft University of Technology, Delft, The Netherlands.

specimens after the healing treatment via visual inspection and crack permeability tests. Additionally, a model is built to obtain a mathematical basis for further choice of optimum healing agent and LWA quantity to be applied in the self-healing mortar. Finally, the results obtained from both experimental and numerical studies are evaluated and recommendations for future research are given. While previous research (Wiktor *et al*. 2011; Tziviloglou *et al*. 2016) has proven (experimentally) the enhanced healing behaviour of the bio-based mortars compared to conventional ones, this paper addresses and compares methodologies exclusively on bio-based specimens.

2. Materials and methods

2.1 Preparation of the healing agent

The bacteria-based healing agent consisted of spores derived from alkaliphilic bacteria of the genus Bacillus and organic mineral compounds. The healing agent is incorporated in LWA (expanded clay particles, Liapor 1/4 mm, Liapor GmbH Germany) via an impregnation under vacuum with calcium lactate- (200 g/L), yeast extract- (4 g/L) and bacteria spores (10^8 spores/L) solution. Following the impregnation, the LWA were dried for approximately 5-6 days at standard temperature (20 ± 2 ˚C) with 60 ± 10% RH, until a constant weight was achieved (Tziviloglou *et al*. 2016). During drying procedure, the spores can remain in dormant state, since the pH of the environment is not adequately high for them to activate and start germinating. It was found that after drying, the impregnated LWA increased their initial weight in average by 11.3%, due to the addition of the healing agent. The increase in weight was measured experimentally in a sample of 40 LWA (20 before and 20 after impregnation). The experiment was held as follows:

- The diameter and the weight of 20 empty LWA was measured before the impregnation procedure.
- After drying, 20 impregnated LWA having the same diameters as the empty LWA used before, were weighted.
- The difference in weight was calculated for each LWA and finally an average value was obtained.

Table 1 Mix design of bio-based mortar.

Compound	Amount (kg/m^3)	Density (kg/m^3)
CEM I	463	3150
Water	231.5	1000
Sand 0.125/1 mm	855	1650
LWA 1/4 mm	283	650

2.2 Preparation and cracking of mortar prisms

9 mortar prisms were prepared containing ordinary Portland cement (CEM I 42.5 N, ENCI, The Netherlands) and 0.125/4 mm sand or 0.125/1 mm sand and the impregnated LWA. The mixture proportions are presented in **Table 1**. The prisms (40 mm x 40 mm x 160 mm) were reinforced with two steel wires (ø 1mm) to avoid complete fracture in two parts during loading and modified with a hole in their centre, as seen in **Fig. 1**. The hole was created by introducing a smooth (greased) metal bar ø 5 mm while casting, which was pulled-out during demoulding. All specimens were demoulded 24 h after casting and kept in a room with standard temperature (20 ± 2 °C) and > 95% RH for 28 days (Tziviloglou *et al*. 2016).

Three-point-bending (with a span of 100 mm) was used for the crack introduction on 28-days-old mortar prisms. A single crack was created in each specimen. A vertical load was applied in the middle of the specimens until the formation of a stable crack. While loading, the crack opening increased constantly by 0.0005 mm/s until it reached approximately 0.4 mm. The crack width was monitored via two Linear Variable Differential Transducers (LVDTs) attached on the front and the back side of the specimens. When the crack width reached 0.4 mm the specimens were slowly unloaded. After unloading, the crack width reduced to approximately 0.27 – 0.36 mm. The depth of the crack was not monitored during bending, but it was observed through microscopic images. Those images revealed that the crack was developed along the whole height of the specimens (larger on the bottom and zero on the top), therefore, the crack depth was almost equal to the height of the specimen, namely, 40 mm.

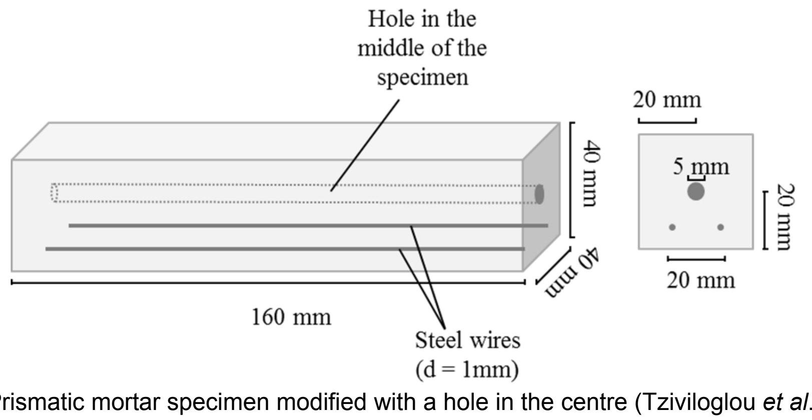

Fig. 1 Prismatic mortar specimen modified with a hole in the centre (Tziviloglou *et al*. 2016).

2.3 Healing treatment

Following the crack creation 6 out of 9 specimens were placed horizontally in a plastic container filled with tap water for crack healing, while 3 of them were immediately tested (crack permeability test). The 6 specimens were completely immersed in water while placed on the top of 10-mm-high spacers. The container was kept open to the atmosphere at standard room temperature (20 ± 2 °C) with (60 ± 10)% RH. 3 out of 6 specimens were left to heal for 28 days, while the other 3 for 56 days. Extra water was added, to keep a constant liquid-to-solid ratio.

2.4 Crack inspection

Crack inspection was used to primarily evaluate the sealing efficiency of the bio-based healing agent. The inspection was conducted in two steps; i.e. right after crack creation and after healing treatment. Images of the cracks were taken by a Leica MZ6 stereomicroscope with a Leica DFC420 camera. Image processing software (ImageJ) was used to estimate the width, the area and ultimately the volume of the crack on the bottom of each specimen. The crack width was calculated as the average of four measurements (w_1, w_2, w_3 and w_4) taken from the bottom of the specimen as seen in **Fig. 2**. In many cases, shape imperfections (rough surface, air voids, etc.), due to casting procedure or poor compaction could cause unexpected local damages after cracking. Therefore, it was decided that the estimation of the crack width should be undertaken by the above described methodology, where the measuring points were predetermined, but they could also be adjusted by the user in case that the point was coinciding with a matrix flaw. In addition, the specific measuring method has also been successfully used in the literature (Wiktor *et al*. 2011; Wang *et al*. 2014; Palin *et al*. 2015).

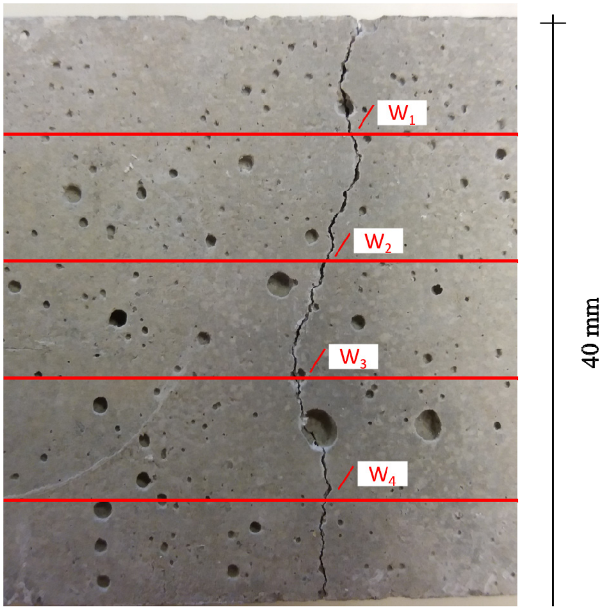

Fig. 2 Measurement of crack width on the bottom of the specimen.

The assessment of crack volume was performed as follows: The images (in grey scale) were thresholded to a grey value of 120 (**Fig. 3**). Afterwards, the crack area (in pixels) was measured and converted to mm^2. In the microscopic images that were taken, the grey values of the mortar matrix and of the healing products were quite similar. Therefore, the thresholded grey value that was used was sufficient to separate and detect the solids (mortar and healing product) from the crack voids. For the estimation of the crack volume it was assumed that the crack had a triangular shape along the height of the specimen. Therefore, the crack volume was estimated by multiplying the crack surface by half of the specimen's height. The sealing percentage α_m (for every specimen) was calculated as in Eq. 1. Where V_i is the initial crack volume and V_t is the crack volume are after healing time *t* (28 or 56 days).

$$a_m = \frac{V_i - V_t}{V_i} \tag{1}$$

2.5 Crack permeability test

Following the crack inspection, the sealing efficiency was studied through a crack permeability test in order to link the functional property (crack permeability) to the visual observations. The test was performed before and after the healing treatment. The set-up of the test is shown in **Fig. 4**.

Since the specimens contained a hole along their length, one of the two end-sides (40 mm x 40 mm) of the sample was sealed with a glue layer to prevent water leakage. A connector was fixed on the other end-side, and a plastic tube was adjusted to it to let the water pass through the 5 mm-hole and leak out of the crack. Under the crack, an electronic scale connected with a computer recorded and plotted the graphs of the mass of the water that leaked from the cracks as a function of time. The test lasted approximately 10 minutes. In all cases the

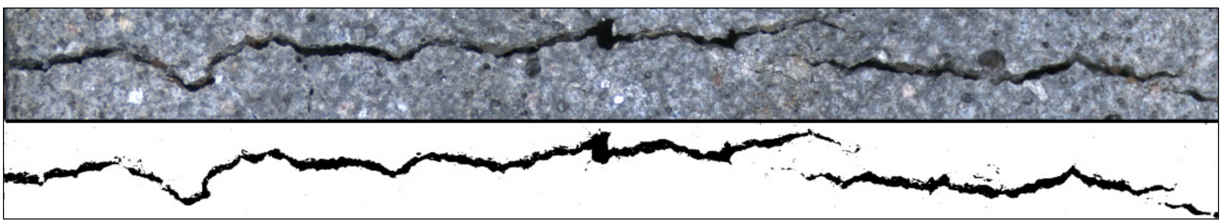
Fig. 3 Crack geometry on the bottom of a specimen.

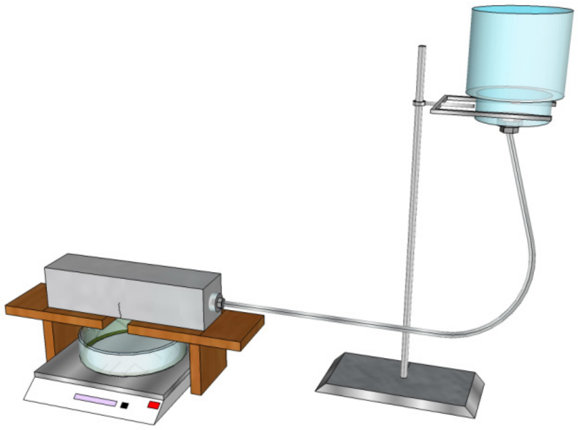

Fig. 4 Crack permeability test set-up on prismatic samples.

relation between the crack flow and time was linear. Therefore, the crack flow of each specimen was calculated as the slope of the resulting curve. The rate (r) of the recovery of water tightness was calculated as seen in Eq. 2. Where f_{n-h} is the average (out of three specimens) crack flow of the non-healed specimens in g/min and f_h is the average (out of three specimens) crack flow of the healed specimens in g/min. Unlike the sealing percentage α_m, the recovery rate r was calculated for the total number of the tested specimens (in this case three). The test was performed before healing treatment on a set of three and after healing on another set. The reason for testing different sets before and after healing was to avoid any loss of healing agent during the first permeability test that could possibly affect the healing process. This fact can influence the obtained results, in a sense that the tested cracks are not identical and might heal differently. Yet, the results can give a good indication for the extend of healing that has taken place during the healing treatment and they could be used for a solid comparison.

$$r = \frac{f_{n-h} - f_h}{f_{n-h}} \tag{2}$$

2.6 Model description

A numerical simulation was conducted at meso-scale to estimate the sealing efficiency of the bacterial-based healing system and to determine the optimized usage of the healing agent. The model used in the simulation was the same as used in the experiments (a 40 mm x 40 mm x 160 mm prism). In the meso-scale model, the mortar (hardened cement paste and sand) and the LWA are taken as a homogeneous matrix and a spherical inclusion, respectively.

To get the meso-scale model of the mortar, the size of each lightweight particle was randomly generated based on the gradation curve which was obtained by a sieve test. The process stops when the volume fraction of all generated LWA reaches the requirement. Then a packing algorithm based on the "take-and-place" method (Wang *et al*. 1999) was adopted to place the LWA into the meso-scale model. During this procedure, a separation check was conducted for each particle to ensure that it was not overlapping with any other particle which already existed in the model. **Figure 5** shows a typical example of the simulated meso-scale model.

Following the creation of the meso-scale model, an artificial V-shaped crack was assumed in the middle of the prism, according to the experimental observations. Based on the size and the position of the LWA, all the lightweight particles which were intersected by the crack could be identified. These LWA were considered as damaged by the crack. Consequently, the healing agent lying inside the pores of the LWA would be released to form the chemical products which can seal the crack. The sealing percentage (α_s) according to the simulation can be expressed generally as in Eq. 3,

$$\alpha_s = \frac{V_{sp}}{V_{cr}} = \frac{V_{cp} \cdot \beta}{0.5 \cdot d_{cr} \cdot w_{cr} \cdot l_y} \tag{3}$$

where V_{sp}, V_{cp} and V_{cr} are the volume of the sealing product, the volume of the cracked particles and the volume of the crack, respectively; d_{cr} is the crack depth which in this case (to compare with the experimental

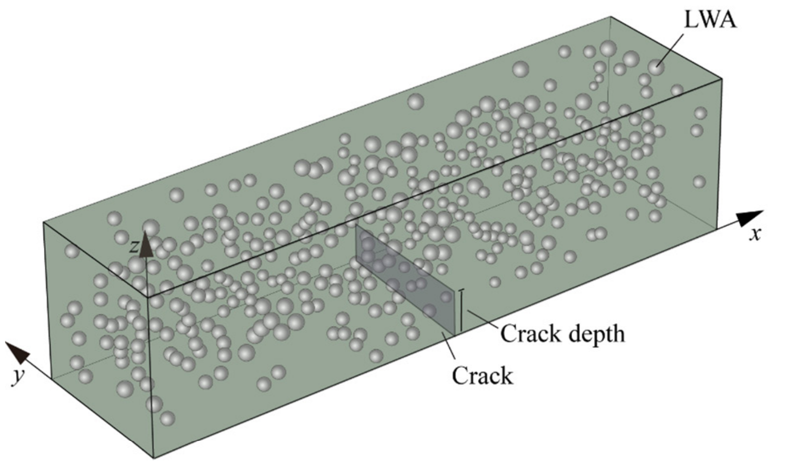

Fig. 5 A schematic of meso-scale model of mortar containing LWA.

results) coincides with the height of the specimen; w_{cr} is the crack width; l_y is the length of the model in the y direction shown in **Fig. 5** and β is a dimensionless parameter which represents the amount of sealing product that can be formed for each unit of volume of LWA. In the simulation of a three-point bending test, the crack is assumed to be initiated in the middle of the specimen, i.e., $x = 0.5l$, where l_x is the model size along the x-direction. It is also assumed that the crack can propagate through a lightweight particle, due to its lower strength compared to a normal aggregate. Thus, the cracked LWA can be identified by checking whether they have been intersected by the crack surface. Then, the total volume of cracked LWA, i.e., V_{cp}, can be calculated according to the diameter of each cracked particle.

The concept of the bacteria-based self-healing concrete indicates that in the presence of oxygen and water inside the crack, the dormant bacterial spores are activated. Later, the active bacteria cells convert the calcium lactate ($CaC_6H_{10}O_6$), present in the healing agent to calcium carbonate by using oxygen. Thus, when the healing agent of the cracked LWA is released into the cement paste, the following chemical reaction will occur (Wiktor *et al.* 2011):

$$CaC_6H_{10}O_6 + 6O_6 \rightarrow CaCO_3 + 5CO_2 + H_2O \tag{4}$$

Carbon dioxide (CO_2) formed during the above reaction can further react with portlandite $Ca(OH)_2$ present in the mortar matrix as a product of cement hydration:

$$Ca(OH)_2 + CO_2 \rightarrow CaCO_3 + H_2O \tag{5}$$

Based on the above chemical reactions, $CaCO_3$ is considered as the product which seals the crack. Thus, β in Equ. 3 can be calculated as:

$$\beta = \frac{\gamma \cdot 650 \cdot 6 \cdot 0{,}10009}{0{,}21822 \cdot 2711} = 0{,}66 \cdot \gamma \tag{6}$$

In Eq. 6, 650 (kg/m^3) is the packing density of the LWA used in the experiment; 0.21822 (kg/mol) is the molar mass of calcium lactate; 0.10009 (kg/mol) and 2711 (kg/m^3) are the molar mass and density of $CaCO_3$, respectively; the coefficient 6 represents the (total) mol of $CaCO_3$ that can be produced by 1 mol of calcium lactate (Eqs. 4 and 5); γ is the mass of the healing agent inside the unit mass of the LWA which is measured in the experiment. Based on a test on several LWA, it was found that γ varies between 1.4 and 38.7. Thus, γ was taken as a random variable following a uniform distribution in [1.41, 38.69].

With the value of β in Eq. 6 the sealing percentage (α_s) can be calculated according to Eq. 3. However, since the meso-scale model is randomly generated, α_s should be considered as a random variable. Hence, in the following part of this paper, not only the average, but also the standard deviation of the sealing percentage was considered. The reason to consider the standard deviation is that this parameter (γ) has a large degree of variation (γ=1.4~38.7). Thus, the simulation is performed in a probabilistic approach. In addition, the standard deviation was also considered, in order to know whether the variation of input parameters can significantly affect the output result.

Table 2 Estimated crack width, volume and closure percentage.

Specimen	Crack width (mm)	Crack volume before healing (mm^3)	Crack volume after healing (mm^3)	α_m (%)
1	0,289	253,98	-	-
2	0,315	287,90	-	-
3	0,266	207,26	-	-
4	0,339	334,22	114,04	65,88
5	0,294	259,32	172,24	33,60
6	0,356	312,5	52,66	83,15
7	0,363	338,92	27,66	91,83
8	0,285	243,78	77,02	68,41
9	0,296	274,74	3,56	98,70

Table 3 Estimated crack width and sealing percentage obtained by the simulations.

Specimen	Crack width (mm)	α_s (%)
4	0,339	60,14 ±3,87
5	0,294	69,38 ±4,27
6	0,356	57,20 ± 3,50
7	0,363	56,23 ±3,63
8	0,285	71,43 ± 4,54
9	0,296	68,70 ±4,24

3. Results

3.1 Crack sealing estimation

The specimens were loaded until the crack opening reached 0.4 mm. However, after unloading the crack width was varying from 0.266 to 0.356 mm, based on the stereomicroscopic observations. **Table 2** shows the measured crack width, the crack volume before and after the healing treatment and the calculated sealing percentage (α_m) based on microscopic observations. Specimens 1, 2 and 3 were used as reference for the crack permeability test, and so were not subjected to healing treatment. Specimens 4, 5, 6 and 7, 8, 9 were submerged in water for 28 and 56 days respectively. It can be stated that crack closure percentage increased for the specimens immersed in water for 56 days in comparison with those immersed for 28 days. The crack width exhibited a linear relation with the crack volume as seen in **Fig. 6**. In contrast with the crack width/volume which does not show a clear relation with the sealing percentage (**Fig. 7**). It could have been expected that the smaller crack volume would lead in more efficient the crack closure. However, this was not concluded from the microscopic observations. **Table 3**

Table 4 Results from crack permeability test on prismatic mortar specimens.

Sample	Crack width (mm)	Water flow f_{n-h} (g/min)	f_h	r (%)
1	0,289	81,12	-	
2	0,315	134,14	-	-
3	0,266	64,7	-	
4	0,339	-	27,46	
5	0,294	-	21,66	69,41
6	0,356	-	38,04	
7	0,363	-	10,9	
8	0,285	-	6,72	91,75
9	0,296	-	5,88	

shows the measured crack width and the sealing percentage (α_s), as derived from the simulations. Contrary to the relation between crack width and α_m, the relation between crack width and α_s is linear (**Fig. 7**). In other words, the model indicates that the narrower the crack the more efficient the sealing.

Table 5 Values for sealing parameters (α_m, α_s and r) for set of specimens immersed for 28 and 56 days in water.

Sealing parameter	Days of immersion 28	56
α_m	60,88	86,31
α_s	62,24	65,45
r	69,41	91,75

3.2 Crack permeability results

The results from the crack permeability test and the recovery of water tightness for the two sets of specimens are presented in **Table 4**. The results from the water flow test on cracked non-healed specimens indicated that a larger crack area resulted in an increased flow. In addition, from the calculation of the recovery of water tightness it was derived that the longer immersion period led in decreased water flow, therefore, a more efficient the sealing.

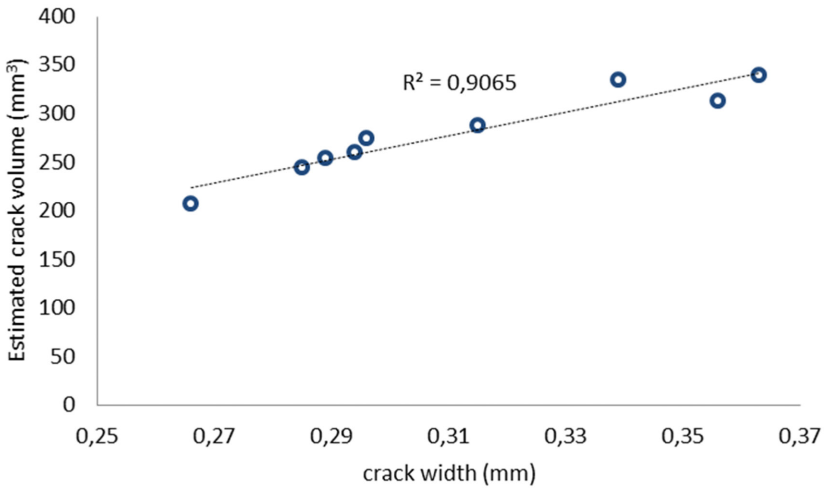

Fig. 6 Estimated crack width-estimated crack volume of mortar specimens.

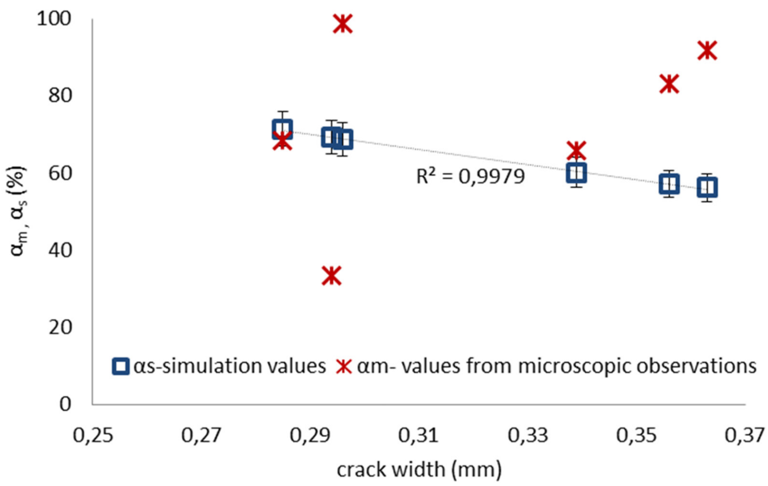

Fig. 7 Estimated crack width - crack closure percentage (microscopic observations) and sealing percentage (simulations).

4. Discussion

This study used three different parameters to evaluate the sealing efficiency of the bio-based self-healing system. All three (α_m, r and α_s) were based on different ways of investigation, namely microscopy observations, crack permeability test and numerical simulations. However, they all specified the sealing efficiency of (a) crack(s) with a certain width. The comparison of α_m and α_s values (**Fig. 7**) revealed that the sealing values obtained by the two different methods are not in good agreement. This can be attributed to the assumptions made for both the crack volume calculations and the numerical simulation. For example, α_m is based on crack volume estimation assuming that the ratio filled-to-empty crack area, along the crack depth, is the same as on the bottom of the specimen. This is probably overestimating the real volume of the $CaCO_3$ in the crack. In addition, (for the calculation of a_s) the model considers that all the healing agent included in the LWA intersected by the crack was released and converted into $CaCO_3$. In reality, only a part of the healing agent is released, while the rest remains in the lightweight particle. Moreover, blockage (from sealing products or from impurities) in the crack can cause depletion of oxygen and therefore limited conversion of the feed into sealing product. Furthermore, in the model, the duration of the immersion period was not taken under consideration, consequently α_s was independent of the healing period. Thus, α_s exhibited roughly similar values for 28 or 56 days of immersion (62.2% and 65.45% respectively, see **Table 5**). The difference in α_s for 28 and 56 days could be exclusively attributed to the different crack widths of the specimens (4, 5, 6 and 7, 8, 9). Finally, the autogenous healing processes, which can take place during water immersion, have not been considered in the simulation. This is an additional reason why the sealing results originating from the model are lower (at least for 56-days-old specimens) than those from the experimental investigation.

Furthermore, the comparison among α_s, α_m and r was conducted for sets of specimens and not separately for each specimen. **Table 5** presents the average values of α_m and α_s, as well as r values for the sets of three specimens immersed in water for 28 and 56 days. In this case, the results of α_m and r are in good agreement for both immersion periods. The α_s average value for 28 days of immersion is similar to the average values of the other two parameters, however, for 56 days the value is significantly lower. In general, r is higher than the average α_m and α_s, since the crack flow test is highly dependent on the crack opening at the position of the hole. Usually at this position (20 mm from the bottom of the specimen) the crack width is narrower than on the bottom and it is more likely to be fully sealed. In this case the real r value is probably overestimated.

Hence, some modifications on the experimental as well as on the computational part are needed to obtain more realistic results. The permeability test results can be improved if the test will be performed on the same set of specimens before and after healing. The danger of losing the healing agent during the first cycle of testing can be avoided by using a liquid with higher pH (possibly carbonate-bicarbonate buffer), where calcium lactate is less soluble. In addition, a straight rather than a V-shaped crack could cause less confusion in the interpretation of the results. Moreover, the image processing could be more accurate if the microscopic observations will be replaced by 3D CT-scanning. Further experimental research should also investigate whether the numerical model needs to include a "reduction factor" which will determine the amount from the initially existed healing agent that participates in crack filling process.

5. Conclusions

In conclusion, this paper summarized three different methodologies to evaluate the sealing efficiency of the bio-based self-healing mortar; two of them were based on experiments (image processing and crack permeability test), while the last one was based on computer simulations. It was concluded that the experimental approaches might overestimate the crack closure due to:

- the hypothesis that the crack filling is constant along the crack length, or
- the fact that the crack permeability test was conducted in different sets of specimens before and after healing treatment, or
- the smaller crack width at the position of the (water passage) hole compared to the crack width on the bottom of the specimens.

In addition, the numerical model results can slightly overestimate the volume of the filling product, due to the assumption that all the healing agent included in the LWA intersected by the crack was released and converted to calcium carbonate. Yet, in general, the model underestimates the total volume of $CaCO_3$ produced in the crack because:

- the duration of the immersion period was not considered as a model variable; therefore, the sealing efficiency was independent of the healing period and
- the autogenous healing processes that occur during the healing treatment in water were also not considered.

As a matter of fact, the reactions that take place inside the crack are quite complex and depend on several factors, such as the (local) crack width, the presence of oxygen, the duration of healing treatment etc. Although both experimental and computational methodologies need some improvements to resemble a more realistic situation, the current approaches can already provide an indication of the crack sealing behaviour originating from the bio-based self-healing system.

Acknowledgements

The authors would like to acknowledge the financial support of European Union Seventh Framework Program (FP7/2007-2013) under grant agreement no 309451 (HEALCON).

References

de Rooij, M., Van Tittelboom, K., De Belie, N. and Schlangen, E., (2013). "Self-healing phenomena in cement-based materials : State-of-the-art-report of RILEM Technical Committee 221-SHC". Dordrecht, The Netherlands, Springer.

Edvardsen, C., (1999). "Water permeability and autogenous healing of cracks in concrete." *ACI materials journal*, 96(4), 448-454.

Feiteira, J., Gruyaert, E. and De Belie, N., (2016). "Self-healing of moving cracks in concrete by means of encapsulated polymer precursors." *Construction and Building Materials*, 102, Part 1, 671-678.

Hearn, N., (1998). "Self-sealing, autogenous healing and continued hydration: What is the difference?" *Materials and Structures*, 31(8), 563-567.

Hilloulin, B., Hilloulin, D., Grondin, F., Loukili, A. and De Belie, N., (2016). "Mechanical regains due to self-healing in cementitious materials: Experimental measurements and micro-mechanical model." *Cement and Concrete Research*, 80, 21-32.

Huang, H. and Ye, G., (2012). "Simulation of self-healing by further hydration in cementitious materials." *Cement and Concrete Composites*, 34(4), 460-467.

Jonkers, H. M., (2011). "Bacteria-based self-healing concrete." *HERON*, 56(1/2), 1-12.

Joseph, C., (2008). "Experimental and numerical study of the fracture and self-healing of cementitious materials." Thesis, (PhD). Cardiff University, UK.

Malm, F. and Grosse, C. U., (2016). "Efficiency of self-healing agents for cementitious materials characterized by NDT." *19th World Conference on Non-Destructive Testing*, 13-17 June 2016, Munich, Germany.

Pacheco, J., Šavija, B., Schlangen, E. and Polder, R. B., (2014). "Assessment of cracks in reinforced concrete by means of electrical resistance and image analysis." *Construction and Building Materials*, 65, 417-426.

Palin, D., Wiktor, V. and Jonkers, H. M., (2015). "Autogenous healing of marine exposed concrete: Characterization and quantification through visual crack closure." *Cement and Concrete Research*, 73, 17-24.

Reinhardt, H. W. and Jooss, M., (2003). "Permeability and self-healing of cracked concrete as a function of temperature and crack width." *Cement and Concrete Research*, 33(7), 981-985.

Roig-Flores, M., Moscato, S., Serna, P. and Ferrara, L., (2015). "Self-healing capability of concrete with crystalline admixtures in different environments." *Construction and Building Materials*, 86, 1-11.

Sangadji, S., (2015). "*Porous network concrete : a bio-inspired building component to make concrete structures self-healing*." Thesis (PhD). Delft University of Technology.

Schlangen, E. and Joseph, C., (2009). "*Self-healing processes in concrete*." In: S. K. Gosh Ed. *Self-Healing Materials: Fundamentals, Design Strategies, and Applications*.Wiley-VCH Verlag GmbH & Co. KGaA : Weinheim, Germany: 141-182.

ter Heide, N., (2005). "Crack healing in hydrating concrete." Thesis (MSc). Delft University of Technology.

Tziviloglou, E., Wiktor, V., Jonkers, H. M. and Schlangen, E., (2016). "Bacteria-based self-healing concrete to increase liquid tightness of cracks." *Construction and Building Materials*, 122, 118-125.

Van Tittelboom, K., De Belie, N., Lehmann, F. and Grosse, C. U., (2012). "Acoustic emission analysis for the quantification of autonomous crack healing in concrete." *Construction and Building Materials*, 28(1), 333-341.

Van Tittelboom, K., Gruyaert, E., Rahier, H. and De Belie, N., (2012). "Influence of mix composition on the extent of autogenous crack healing by continued hydration or calcium carbonate formation." *Construction and Building Materials*, 37, 349-359.

Wang, J., De Belie, N. and Verstraete, W., (2012). "Diatomaceous earth as a protective vehicle for bacteria applied for self-healing concrete." *Journal of Industrial Microbiology and Biotechnology*, 39, 567-577.

Wang, J., Dewanckele, J., Cnudde, V., van Vlierberghe, S., Verstraete, W. and de Belie, N., (2014). "X-ray computed tomography proof of bacterial based self-healing in concrete." *Cement and Concrete Composites*, 53, 289-304.

Wang, Z. M., Kwan, A. K. H. and Chan, H. C., (1999). "Mesoscopic study of concrete I: generation of random aggregate structure and finite element mesh." *Computers & Structures*, 70(5), 533-544.

Wiktor, V. and Jonkers, H. M., (2011). "Quantification of crack-healing in novel bacteria-based self-healing concrete." *Cement and Concrete Composites*, 33(7), 763-770.

Zemskov, S. V., Jonkers, H. M. and Vermolen, F. J., (2011). "Two analytical models for the probability characteristics of a crack hitting encapsulated particles: Application to self-healing materials." *Computational Materials Science*, 50(12), 3323-3333.